Natural Hazards (2024) 120:3429–3446
https://doi.org/10.1007/s11069-023-06346-7

ORIGINAL PAPER

Structural response of cable-stayed bridges exposed to strong earthquakes during construction

Alemdar Bayraktar[1] · Altok Kurşun[2] · Arif Erdiş[2] · Mehmet Akköse[1] · Yavuzhan Taş[3] · Tony T. Y. Yang[4]

Received: 25 January 2023 / Accepted: 16 November 2023 / Published online: 6 December 2023

Abstract
This paper investigates the earthquake response of the Kömürhan cable-stayed bridge with a single pylon and steel deck, which was exposed to the Elazığ-Sivrice earthquake (Mw = 6.8) on January 24, 2020, while it was under construction. The distance from the epicenter to the bridge is approximately 23 km. 82% of the Kömürhan bridge deck was completed during the Elazığ-Sivrice earthquake in 2020. The spectral accelerations of the Elazığ-Sivrice earthquake are approximately 2.5 times greater than those of the design earthquake (72-year) considered during the construction stage. This paper first presents the characteristics of the Kömürhan cable-stayed bridge and the Elazığ-Sivrice earthquake (Mw = 6.8). Subsequently, a 3D numerical finite model of the Kömürhan cable-stayed bridge under construction is created. Modal and seismic responses of the deck, pylon and cables of the bridge under construction are compared for the load combinations including the design (72-year) and the Elazığ-Sivrice earthquakes. The result shows that under the 2020 Elazığ-Sivrice earthquake, the maximum vertical displacements, axial forces, and bending moments of the deck, as well as the cable forces, are three times greater than the design values (72-year). Nevertheless, despite the significant increase in the structural response, no visual damage was observed on the structural elements. This highlights the conservative design of the Kömürhan cable-stayed bridge.

Keywords Cable-stayed bridge · Earthquake response during construction · Structural evaluation · Elazığ-Sivrice earthquake (24 January 2020 Mw = 6.8)

1 Introduction

Cable-stayed bridges consist of three main structural components: the deck, pylons, and inclined cables. They are generally constructed using the cantilever erection method, which fully employs segmental balanced cantilever techniques to build on both sides of the pylon simultaneously (Gimsing and Georgakis (14), Svensson (38)). Due to the complex geometric nature, the positioning of contractor's machinery and equipment on the deck, the construction methods employed, and the dynamic properties of cable-stayed bridges, as well as the characteristics of the excitations, internal forces, stresses, cable forces, and

Extended author information available on the last page of the article

displacements undergo significant changes at each stage of construction. Thus, it becomes imperative to comprehensively understand the system's behavior at each construction stage. Performing detailed analyses at each construction stage are essential in order to preempt unforeseen issues.

Numerous studies concerning the responses of completed cable-stayed bridges under various effects can be found in the references, including the literature survey (Li and Ou (22), Camara (7), Martins et al. (24)). The numerical and experimental studies including construction stage analyses of cable-stayed bridges under earthquake and the other effects are presented below. Wang et al. (43) have investigated numerical responses of cable-stayed bridge at different erection stages during construction using the cantilever method. Su et al. (37) have implemented wind-induced vibration analysis of a cable-stayed bridge during erection by a modified time-domain method. Wilson and Holmes (44) have examined seismic vulnerability and mitigation of cable-stayed bridges during construction. Morgenthal and Yamasaki (26) have explored aerodynamic behaviors of very long cable-stayed bridges during construction. Pipinato et al. (31) have performed the analyses of cable-stayed bridges at different erection stages during construction, assuming the full or the partial cantilever method and performing multiple finite element computational procedure. Atmaca and Ateş (3) have investigated construction stage analysis of three-dimensional cable-stayed bridges. Deng and Liu (12) have carried out the nonlinear stability analysis of a composite girder cable-stayed bridge with three pylons during construction. Lee et al. (21) have determined ultimate experimental and analytical behaviors of cable-stayed bridges under construction. Chengfeng et al. (11) have investigated numerical behaviors of long-span cable-stayed bridges in the construction phase. Park et al. (29) have performed construction stage analysis of cable-stayed bridges using the unstrained element length method. Purohit and Bage (32) have modeled and analyzed Nagpur cable-stayed bridge under construction. Responses of cable-stayed bridges considering geometric nonlinearity, construction stages and time dependent material properties have been searched by Patel et al. (30). Kim et al. (17) have obtained the stability characteristics of steel cable-stayed bridges during construction. Yadi et al. (45) have performed shake table tests of a floating cable-stayed bridge under earthquake excitation during construction with the balanced cantilever method. Granata et al. (16) have implemented construction sequence analyses of long-span cable-stayed bridges. Kim et al. (18) have determined ultimate behavior of steel cable-stayed bridges under construction using a three-step analysis consisting of initial shape analysis, construction stage analysis and external load analysis. Ma et al. (23) have carried out the aerodynamic characteristics of a long-span cable-stayed bridge under construction.

In addition to these, researchers have also investigated the real responses of completed cable-stayed bridges during earthquakes. Filiatrauit et al. (13) have examined experimental and nonlinear numerical dynamic behavior of the cable-stayed Shipshaw bridge during 1988 Saguenay earthquake. Chang et al. (10) have determined the dynamic behavior of the Chi-Lu cable-stayed bridge during the 1999 Taiwan earthquake. Dynamic behavior of Yokohama-Bay Bridge under six earthquakes has been evaluated by Siringoringo and Fujino (34). Siringoringo and Fujino (35) have identified the dynamic characteristics of a curved cable-stayed bridge from strong ground motion records. Seismic response of the Yokohama Bay cable-stayed bridge during the 2011 great east Japan earthquake has been investigated by Siringoringo et al. (36). Bayraktar et al. (4) have monitored structural performance of Nissibi cable-stayed bridge during the main and aftershocks of Adıyaman-Samsat earthquake on March 2, 2017. Yi and Li (48) have determined seismic response of inclined tower legs of cable-stayed bridges during earthquakes.

However, there have been very few investigations into the real earthquake effects on the long-span bridges under construction (Tada et al. (39), Nasu and Tatsumi (27), Yamagata et al. (46), Goto et al. (15), Yasuda et al. (47), Okuda et al. (28). These studies are related to the Akashi Kaikyo long-span suspension bridge. During its construction, the Akashi Kaikyo long-span suspension bridge faced the significant Hyogoken-Nanbu (Kobe) earthquake on January 17, 1995, with a magnitude of 7.2. The earthquake's epicenter was close to the Akashi Kaikyo Bridge. At the time of the earthquake, the tower erection had been completed, all strands for the main cables were positioned, and cable squeezing work was underway, preparing for the stiffening girders' installation. Various methods were employed to investigate the earthquake's impact on the bridge, including visual inspections of the bridge's structural elements and the surrounding ground around the main tower foundations, geological surveys, underwater cameras, relative displacement measurements using geometrical methods, stress analysis of cables and towers, as well as velocity records obtained at the top and middle levels of the towers (Tada et al. (39), Nasu and Tatsumi (27), Yamagata et al. (46), Goto et al. (15), Yasuda et al. (47), Okuda et al. (28)). No damage was sustained by the main structures that had already been erected, which encompassed elements like the anchorages, tower foundations, towers, and cables. The survey findings revealed that the main tower foundation on the Awaji Island side (3P) had undergone a relative displacement of approximately 1.3 m in a westerly direction, while the Awaji Island anchorage (4A) had similarly shifted about 1.4 m to the west. Consequently, the center span extended from 1990 m to roughly 1990.8 m, and the side span on the Awaji Island side also grew from 960 m to approximately 960.3 m.

This paper aims to investigate the 3D seismic behavior of long-span cable-stayed bridges encountered to earthquakes during the construction stage. Kömürhan cable-stayed bridge with a single pylon and steel deck in Turkey is selected as an application. The bridge was exposed to the Elazığ-Sivrice earthquake on January 24, 2020 (Mw = 6.8) while under construction, with 82% of the construction completed at the time of the earthquake. The spectral accelerations of Elazığ-Sivrice earthquake were approximately 2.5 times greater than those of the 72-year earthquake considered in the construction stage analysis of the bridge. In this paper, the characteristics of Kömürhan cable-stayed bridge and Elazığ-Sivrice earthquake (Mw = 6.8) are first presented. Then, a 3D model is developed and utilized to examine the seismic behavior of the bridge during construction, considering different load combinations from both the design (72-year) earthquake and the Elazığ-Sivrice earthquake.

2 Structural characteristics of the Kömürhan bridge under construction

The Kömürhan cable-stayed bridge was constructed over the Karakaya Dam across the Euphrates River in Southeastern Anatolia. It is part of the Malatya-Elazığ State Highway and officially opened for service on January 2, 2021. The bridge is 660 m in length and was designed as cable-stayed with a single inverted Y pylon of 165.5 m high. Since the bridge has a single pylon, unlike general applications, the deck was built by advancing in the form of a console from one side. The pylon is made of reinforced concrete. The lengths of main span, the back span anchorage block and approaching viaduct are 380 m, 180 m, 100 m, respectively. The steel deck cross section of main span is orthotropic. The width and height of the steel deck are 23.86 m/25.00 m and 3.59 m, respectively. The superstructure of the

bridge is connected to the pylon with 42 tensioned cables. The cable system consists of the typical 7 wire 0.6″ galvanized strand, and the cable cross sections vary depending on the force in the stay cable. The cross section, ultimate force, ultimate strength and yield strength of each strand used in the cables and tendons are 150mm^2, 279kN, 1860 N/mm^2 and 1600N/mm^2, respectively (Bayraktar et al. (5)). The steel classes of main span and prestressed concrete are S355 J2 and S500a, respectively (AASHTO LRFD (1), Eurocode 3 (CEN 9)). The concrete class of the pylon is C50/60 (Eurocode 2 (CEN 8)). While the reinforced concrete deck of the approaching viaduct is designed as C40/50, concrete class of and back span anchorage block, pylon foundation and abutments are designed with C30/37 (Eurocode 2 (CEN 8)). The geological formation of bridge location consists of serpentinite rocks common in the Kömürhan Ophiolites region (Kömürhan Bridge Project, 20). The pylon foundation, which is located in Malatya side, sits on two caissons with diameter and depth of 15 m and 22.5 m, respectively.

During the 24 January 2020 Elazığ-Sivrice earthquake (Mw = 6.8), the Kömürhan bridge was under construction. Views and sections of Kömürhan cable-stayed bridge under construction are shown in Fig. 1. The distance from the epicenter of the earthquake to the Kömürhan Bridge is approximately 23 km. When the Elazığ-Sivrice earthquake occurred, 82% (262 m of the main span) of the bridge deck, which corresponds to 542 m of the 660 m total bridge length, has been completed during the earthquake. However, 16 of the 42 cables in the bridge have not been connected.

3 Characteristics of the Elazığ-Sivrice earthquake (Mw = 6.8)

The Kömürhan cable-stayed bridge is situated close to the Eastern Anatolian Fault Zone (EAFZ), which is one of the active fault systems on which many destructive earthquakes have occurred in the history. The East Anatolian Fault Zone (EAFZ) is defined by a zone of fault segments that joins the eastern end of the North Anatolian Fault Zone (NAFZ) to the Mediterranean Sea in the Gulf of Iskenderun. Earthquake activity that occurred during the historical and instrumental period throughout EAFZ is shown in Fig. 2. Significant seismic events in the area include the 1905 Pütürge-Maltya (6.8), 1908 Malatya (6.1), 1964 Sincik-Adıyaman (6.0), 1966 Karlıova-Bingöl (6.2), 1971 Bingöl (6.8), 1975 Lice-Diyarbakır (6.6), 1986 Doğanşehir-Malatya (6.0), 2003 Pülümür-Tunceli (6.3), 2010 Kovancılar-Elazığ (6.1) earthquakes, 2023 Kahramanmaraş-Pazarcık (7.7) and Kahramanmaraş-Elbistan (7.6). The Elazığ-Sivrice earthquake (Mw = 6.8) occurred on January 24, 2020 (AFAD, 2).

The Elazığ-Sivrice earthquake with magnitude of 6.8 (Mw) took place near the Sivrice district of the Elazığ province at 20:55:11 (UTC) local time on January 24, 2020. The mainshock was followed by 1948 aftershocks with magnitudes ranging in between 0.8 and 5.1, within 10 days after the event. It can be seen from Fig. 3 that the earthquake occurred on the East Anatolian Fault zone, due to a NE-SW strike-slip fault rupture along the Sivrice-Pütürge Segment in Elazığ, Turkey (AFAD (2), METU (25), KOERI (19)). The epicenter is located at N38.3593°, E39.0630°, approximately 40 km southwest of Elazığ, and 64 km east of Malatya with a focal depth of 8.06 km (AFAD, 2). The effects of the Elazığ-Sivrice earthquake have been widely observed across Elazığ and Malatya regions, extending from Hazar Lake in the east to downtown Malatya in the west. The cities of Kahramanmaraş, Diyarbakır, Adıyaman, Şanlıurfa and Batman have also felt the earthquake shaking strongly (Fig. 4). It can be seen from Fig. 4 that the closest station is Sivrice

a) Views

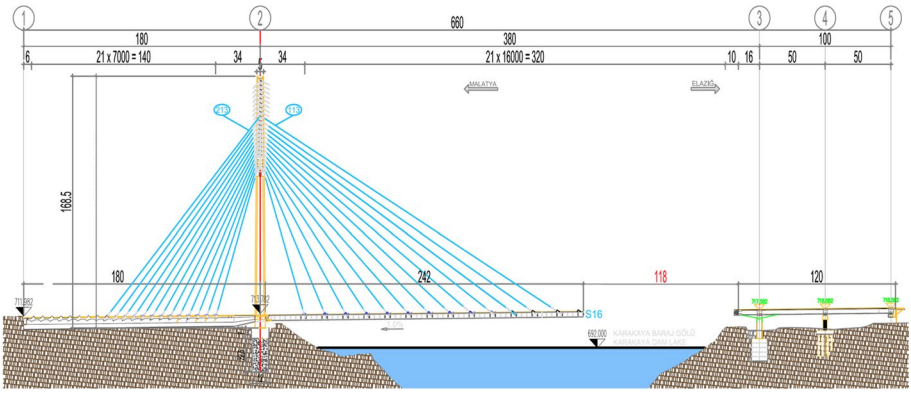

b) Longitudinal section (units in m)

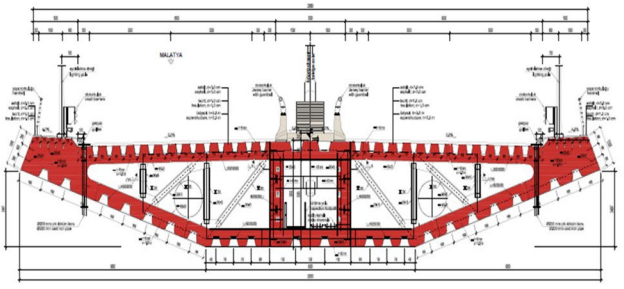

c) Cross section

Fig. 1 Views and sections of Kömürhan cable-stayed bridge under construction (Kömürhan Bridge Project, 20)

(2308), which sits practically on the fault and has a 23 km epicentral distance. The distance from the epicenter to the Kömürhan bridge is approximately 23 km. The epicenter is approximately equidistant from both station 2308 and the bridge. The bridge is oriented approximately in the north-east to south-west direction. Acceleration records taken from Sivrice station (2308) are depicted in Fig. 5. Largest peak ground acceleration (PGA) values are given in Table 1. The raw peak ground acceleration at this station 0.298 g, which at the same time is the largest recorded acceleration during this event. Since maximum

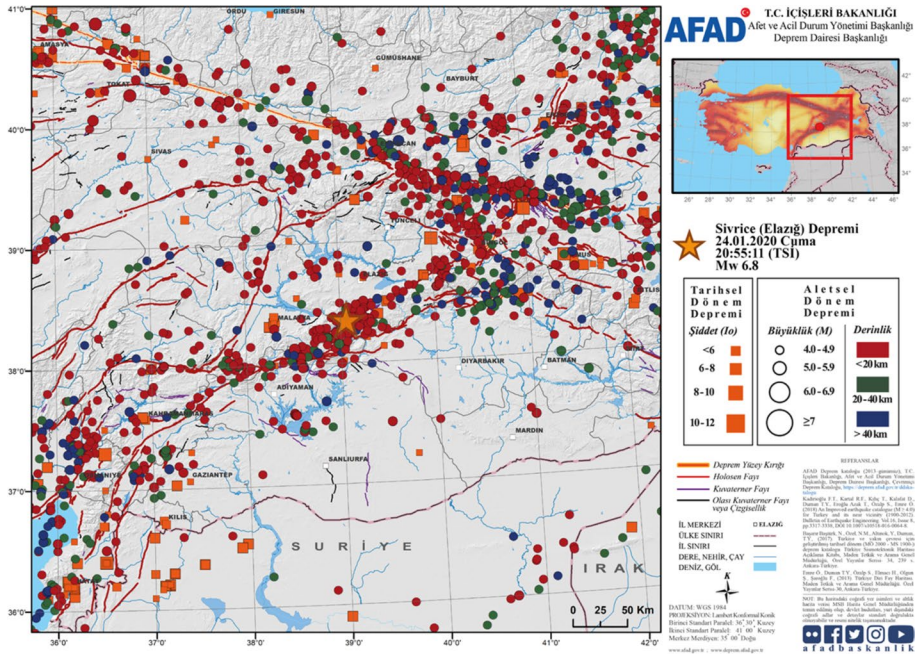

Fig. 2 Earthquake activities of the EAFZ in the historical and instrumental period (AFAD, 2)

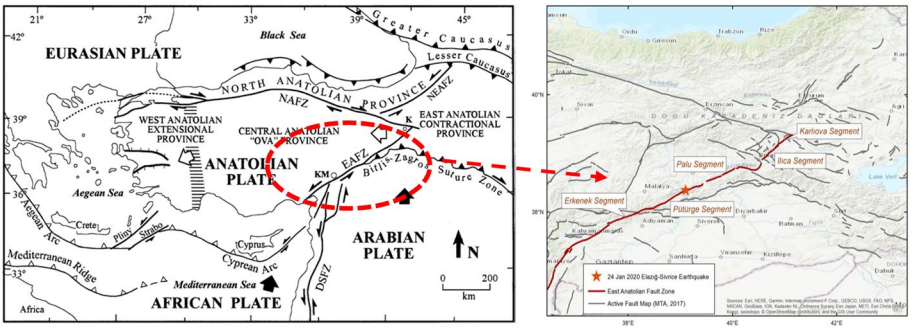

Fig. 3 Tectonic structure of Turkey and the Elazığ-Sivrice earthquake and its relationship with the segments East Anatolian Fault Zone (Bozkurt (6), KOERI (19))

peak ground acceleration occurred in the east–west direction, the east–west component is selected for the earthquake analyses.

Seismic-resistant structures are designed to have the capacity to resist (i) frequent (with return period 50–100 years) minor earthquakes without damage, (ii) infrequent (with return period approximately 500 years) moderate earthquakes with limited structural and nonstructural damage, and (iii) very strong and rare earthquakes (with return period approximately 2500 years) without collapse and life safety endangerment (Tsompanakis, 41). For more critical infrastructure, even higher seismic demand levels are

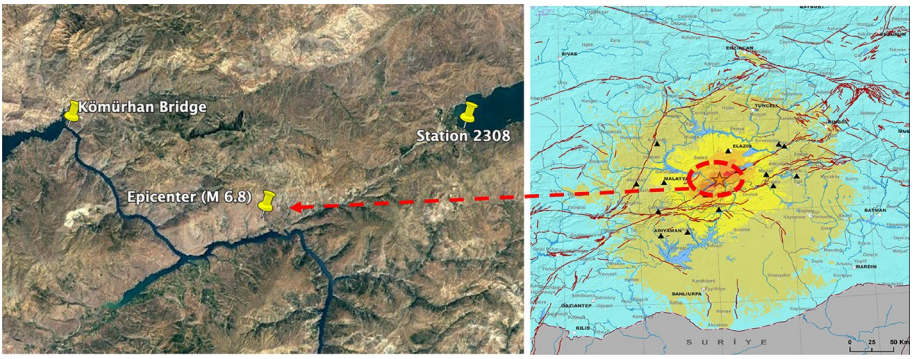

Fig. 4 Locations of the epicenter, the Sivrice station and the Kömürhan bridge (AFAD, 2)

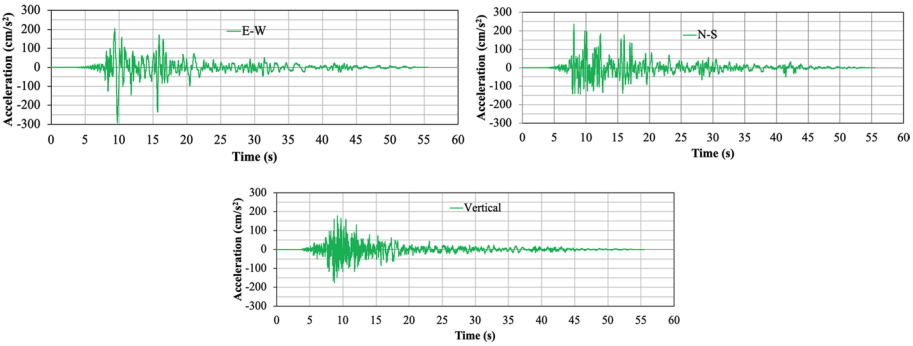

Fig. 5 Acceleration records taken from Sivrice station (2308) (URL-1, 42)

Table 1 Largest peak ground acceleration (PGA) value and epicentral distance taken from the Sivrice station (URL-1, 42)

Station							PGA (cm/s^2)			Depth (km)
Province	Town	Code	Latitude	Longitude	V_{s30} (m/s)	Soil Class	N–S	E–W	U–D	
Elazığ	Sivrice	2308	38.451	39.310	450	ZC	238	292.8	190.1	8.06

imposed which is interpreted in terms of a very large return period, such as 10,000 years for maximum design earthquake motions for major dams.

The design earthquakes have a probability of exceedance of the 50% in 50 years (72 years return period) for the construction stages and 2% (2475 years return period) in 50 years for completed stage. It is assumed that the bridge will behave elastically for 2% in 50 years hazard level where damage in the pylon and foundation will not be allowed. The peak ground accelerations of 50% (72-year) and 2% (2475-year) earthquakes were taken as 0.15 g and 0.5 g, respectively (Kömürhan Bridge Project, 20). The Turkish Earthquake Code (TEC) published in 2007 (TEC, 40) was considered, and the smoothed design acceleration spectra were utilized in the design phase of the Kömürhan

Bridge (Kömürhan Bridge Project, 20). The spectrum comparisons between the design (for return periods of 72 and 2475 years) and the Elazığ-Sivrice earthquake recorded at the Sivrice station (2308) are depicted in Fig. 6. The comparisons are presented for the East–West (E-W), North–South (N-S), and Vertical (V) components, considering a damping ratio of 5%. Peak spectral acceleration values of design spectrums for 2475-year and 72-year return periods are equal 1.26 g and 0.37 g, respectively. It can be seen from Fig. 6 that the maximum spectral accelerations for E-W, N-S and vertical components in Elazığ-Sivrice station are 0.79 g, 0.89 g, 0.74 g, respectively. Maximum spectral values of Elazığ-Sivrice earthquake components are significantly greater than those of 72-year design earthquake considered for the construction stage. It can be stated that the spectral values of Elazığ-Sivrice earthquake components coincide with an earthquake of approximately 475-year return period.

4 Visual inspection of the Kömürhan bridge after the Elazığ-Sivrice earthquake

The 16th segment of the bridge deck (82% of the total length) was constructed during the Elazığ-Sivrice earthquake. Observational inspections conducted on the critical areas of the bridge and its structural elements after the earthquake (YP, 49). Figure 7 indicates that no damage has been observed at the foundation connections of the pylon on both the Elazığ and Malatya sides. Additionally, no deformations or cracks were detected at the junction point of the inclined legs of the pylon with the composite single section of the tower. Visible cracks or deformations had not been observed in the shear keys, uplift points, supports, cap beams, and piers (Fig. 8).

At the connection point of the steel box section with the reinforced concrete section, no deficiencies had been observed in the anchorage elements, both transversely and longitudinally (Fig. 9). It can be seen from Fig. 10 that no deficiencies had been encountered in the cable anchor regions within the segment and back span anchorage block after the earthquake. Additionally, any deviation or change in the positions of the centers where the cables exit through the formwork tube has not been observed.

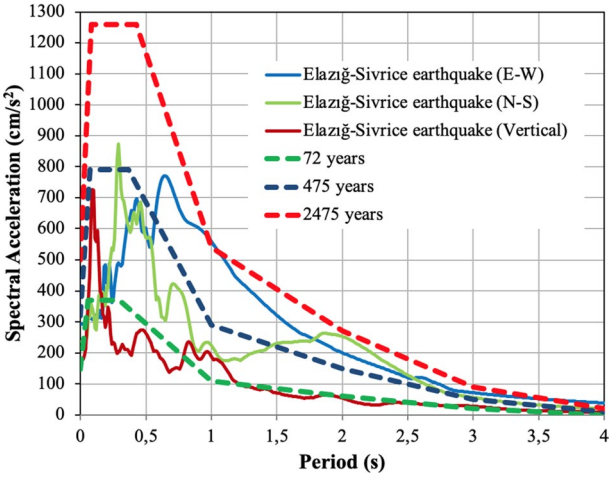

Fig. 6 Spectrums of the design (for return periods of 72 and 2475 years) and Elazığ-Sivrice earthquake at the Sivrice station (2308)

Fig. 7 Views from the foundation connection of the pylon on the Elazığ and Malatya sides

Fig. 8 Views from the shear keys, uplift points, supports, cap beams and piers

Fig. 9 Views from the anchorage elements at the connection point

Deformations and buckling had not been observed in the elements and U-ribs (Fig. 11). Furthermore, at the segment connection junctions, no deficiencies had been observed in the condition of the elements and welds oriented along the segment.

Fig.10 Views from the cable anchor regions

Fig. 11 Views from the steel segments and connections

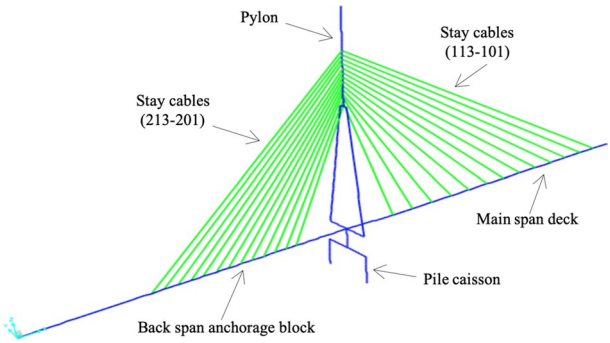

Fig. 12 Finite element model of the Kömürhan cable-stayed bridge under construction

5 Dynamic responses of the Kömürhan bridge under construction

Modal and earthquake responses of the Kömürhan cable-stayed bridge under construction have been simulated numerically. The 3D finite element model of the bridge under construction was created in SAP2000 (33) is shown in Fig. 12. The 3D frame elements were used in the 3D modeling of foundation, back span anchorage block, main span deck and pylon. Cable elements were utilized for the stay cables. The dimensions and material properties of the structural elements of the bridge are mentioned in Sect. 2.

5.1 Modal behavior of the bridge under construction

In the earthquake analyses of the Kömürhan Bridge under construction, the first two hundred modes were considered. The mass participation ratio for the first two hundred modes is 90.27%. The first six mode shapes and periods determined from the modal analysis of the bridge are shown in Fig. 13. The periods of the first six modes vary between 3.09 s and 0.76 s. When the spectrum curve of the E-W component of the Elazığ-Sivrice earthquake given in Fig. 6 is examined, the values of spectral accelerations under period of 3 s are considerably greater than those of the design earthquake (72-year) values considered for the construction state. It can be seen from Fig. 13 that the first mode of Kömürhan cable-stayed bridge under construction shows deck transverse response. In the second and third modes, the deck moves vertically, while the middle part of the pylon moves longitudinally. The fourth mode shows pylon transverse response. In the fifth and sixth modes, the deck moves vertically, while the pylon moves longitudinally. Total modal participating mass ratio of the first six modes is 19.42%

5.2 Earthquake response of the bridge under construction

The Response Spectrum Method was employed in this study, since this method was used in the design of the bridge for construction stage (Kömürhan Bridge Project, 20). The spectrum curves of design earthquake (72-year) and the E-W component of Elazığ-Sivrice earthquake shown in Fig. 6 are considered for the earthquake analyses. Four different load combinations have been considered in analyzing the structural response of the bridge model under construction. The selected load combinations are i) EQ-72: X + 0.3Y, ii) EQ-72: 0.3X + Y, iii) EQ-Elazığ-Sivrice: X + 0.3Y, iv) EQ-Elazığ-Sivrice: 0.3X + Y, where EQ-72 and EQ-Elazığ-Sivrice sembolize design earthquake (72-year)

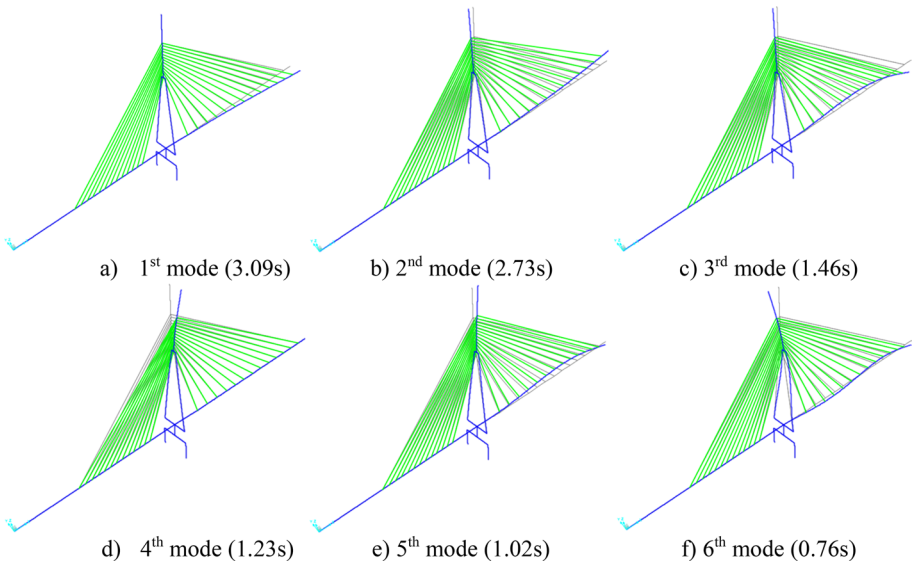

Fig. 13 The first six mode shapes and periods of the Kömürhan cable-stayed bridge under construction

and E-W component of the Elazığ-Sivrice earthquake, respectively, where X and Y represent the longitudinal and transverse directions. The maximum values of the displacements and internal forces occurred on the pylon and main span deck, and cable forces of the Kömürhan bridge model under construction are obtained for the different load combinations above. Since 5% of damping ratio was taken into account in the design of the Kömürhan bridge (Kömürhan Bridge Project, 20), the identical damping ratio was selected for the comparison of the design results with the responses to the Elazığ-Sivrice earthquake.

The variations of the absolute maximum displacements along the main span deck and height of the pylon for the load combinations including the design (72-year) and the Elazığ-Sivrice earthquake are compared in Fig. 14. It can be seen from Fig. 1b that 242 m of the main span steel deck was completed during the Elazığ-Sivrice earthquake, while whole of the reinforced concrete pylon was built. An abrupt change is observed on the vertical displacements of the deck. It is thought that this change stems from the intricate behavior of the mode shapes of the deck under construction. The differences in the displacement curves of the main span deck and the pylon increase with considering the Elazığ-Sivrice earthquake in load combinations. While absolute maximum deck vertical displacements are calculated as 109.9 mm and 336. 6 mm for EQ-72:X + 0.3Y and EQ-Elazığ-Sivrice:X + 0.3Y load cases, the maximum longitudinal displacements on the top of the pylon are obtained as 53.5 mm and 206.5 mm, respectively. The Elazığ-Sivrice earthquake increases maximum values of the vertical displacements of the main span steel deck by 3 times and the longitudinal displacements of the pylon by 3.9 times compared to the design earthquake (72-year). However, after the earthquake, residual movements were not observed along the deck and pylon. Besides, this situation has been confirmed by the field measurements. According to daily measurements in the back span anchorage block, no settlement was measured after the Elazığ-Sivrice earthquake. In addition, there was no difference between the project values of the deck and pylon geodetic measurements before and after the Elazığ-Sivrice earthquake. The elevation differences of the segment 16, which is the last constructed segment, at the deck center on December 22 and December 25, 2020, were surveyed as 0.326 m and 0.324 m, respectively. The geodetic measurement differences of the pylon top along the longitudinal direction before and after the Elazığ-Sivrice earthquake are 0.326 m and 0.327 m, respectively. Since the monitoring system equipped with various sensors for the Kömürhan Bridge was established after its construction (Bayraktar et al. 5), a comparison of sensor data during the construction phase was not feasible.

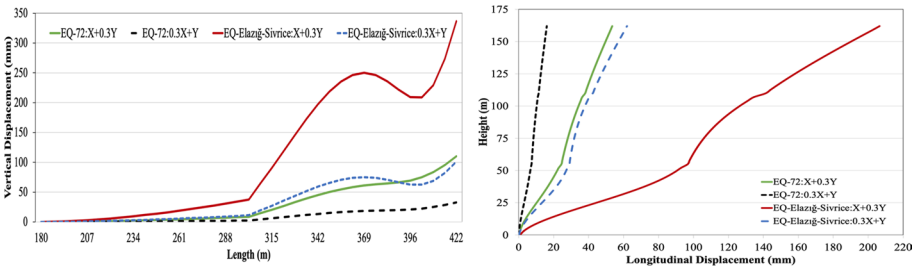

a) Main span deck vertical displacements b) Pylon longitudinal displacements

Fig. 14 Comparison of displacements along the main span deck (a) and pylon (b) for the load combinations including the design (72-year) and the Elazığ-Sivrice earthquakes

The variations of the absolute maximum axial forces and bending moments along the main span deck for the load combinations including the design (72-year) and the Elazığ-Sivrice earthquakes are compared in Fig. 15. According to the design earthquake (72-year), the Elazığ-Sivrice earthquake significantly affects the variations and values of axial forces and bending moments along the main span deck. Absolute maximum axial forces and bending moments obtained in the main span deck for the EQ-72:X + 0.3Y and EQ-Elazığ-Sivrice:X + 0.3Y load combinations are 9620kN, 17741kN, and 17640kNm, 80220kNm, respectively. The Elazığ-Sivrice earthquake increases maximum values of the axial forces and bending moments in the main span steel deck by 1.84 and 4.55 times of the design earthquake (72-year). Observation and ultrasonic tests were implemented on the main span steel deck after the Elazığ-Sivrice earthquake. No damage was observed in the welding of the deck segment connections after the earthquake. It was evaluated that there was no damage in the bridge during the Elazığ-Sivrice earthquake due to the console behavior of the deck and the designing of the structural elements conservatively.

The comparisons of the absolute maximum axial and shear forces and bending moments along the middle part of the pylon for the design (72-year) and the Elazığ-Sivrice earthquakes are shown in Fig. 16. While absolute maximum axial forces at bottom of the middle part of the pylon are calculated as 3313kN and 10698kN for the EQ-72:X + 0.3Y and EQ-Elazığ-Sivrice:X + 0.3Y load cases, the bending moments are obtained as 79,260 kNm and 340,100 kNm, respectively. Maximum values of the axial forces and bending moments obtained for the Elazığ-Sivrice earthquake in the middle part of the pylon increase by 3.2 and 4.3 times compared to the design earthquake (72-year). When the basic connection

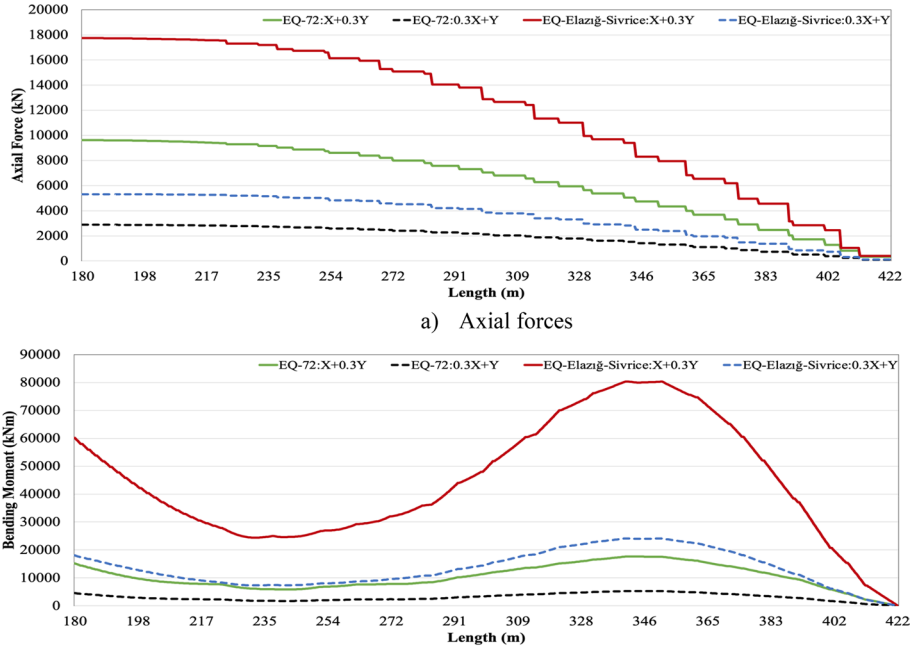

Fig. 15 Comparison of axial forces and bending moments along the main span deck for the load combinations including the design (72-year) and the Elazığ-Sivrice earthquakes

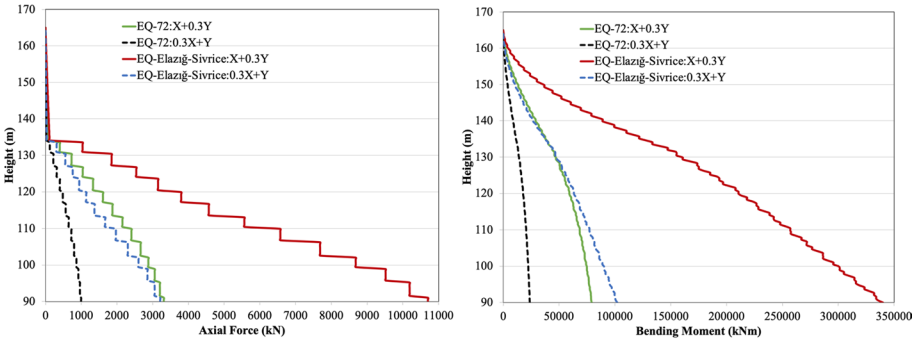

a) Axial forces b) Bending moments

Fig. 16 Comparison of axial forces and bending moments along middle part of the pylon for the load combinations including the design (72-year) and the Elazığ-Sivrice earthquakes

points of the pylon were examined after the Elazığ-Sivrice earthquake, no deformation or cracks were detected at the middle part connection point of the inclined legs and the pylon-deck interfaces.

The variations of the cable forces in the main span deck and back span anchorage block for the load combinations including design (72-year) and the Elazığ-Sivrice earthquakes are plotted in Fig. 17. It can be seen from Fig. 17 that during the Elazığ-Sivrice earthquake,

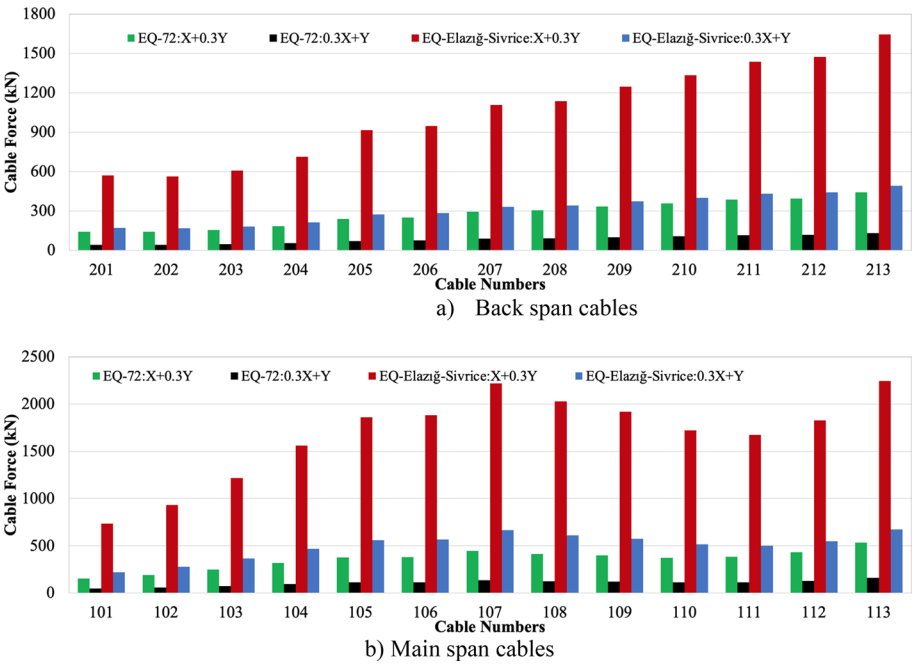

a) Back span cables

b) Main span cables

Fig. 17 Comparison of cable forces obtained for the load combinations including design (EQ-72) and Elazığ-Sivrice earthquakes

both the back span anchorage block and main span cable forces significantly vary and increase according to the design earthquake (72-year). Maximum cable forces occur in the longest cables, 213 (back span, number of the strands 109 and $\alpha = 49.19°$) and 113 (main span, number of strands 85 and $\alpha = 30.36°$), of the back span anchorage block and main span deck. While absolute maximum forces in Cable 213 are calculated as 441kN and 1645kN for EQ-72:X + 0.3Y and EQ-Elazığ-Sivrice:X + 0.3Y, the forces in Cable 113 are obtained as 533kN and 2244kN. The allowable stress in cables is 0.45 times ultimate value. Cable forces calculated for the four load cases are within allowable limits. Measurements on the cable sags also were implemented after the Elazığ-Sivrice earthquake. According to the sag measurements after the Elazığ-Sivrice earthquake, there was no difference between the project and constructed values. Besides, a deviation in the centers of the cables and a damage in the cable anchorages of the main span, the back span anchorage block and the pylon were not observed after the Elazığ-Sivrice earthquake.

6 Conclusions

The effect of the 24 January 2020 Elazığ-Sivrice earthquake (Mw = 6.8) on the structural response of the Kömürhan cable-stayed bridge with steel deck under construction has been investigated in this study. The distance from the epicenter to the bridge is approximately 23 km, and 82% of the bridge deck was completed during the earthquake. The results related to structural performances of the deck, pylon, cables and connections of the bridge under construction are summarized:

- The values of spectral acceleration of the Elazığ-Sivrice earthquake are approximately 2.5 times of the bridge design spectrum (72-year) considered in the construction stage analyses. The Elazığ-Sivrice earthquake increases the vertical displacements of the main span steel deck and the longitudinal displacements of the pylon as 3.06 times and 3.86 times, respectively.
- The Elazığ-Sivrice earthquake increases maximum values of the axial forces and bending moments in the main span steel deck by 1.84 and 4.55 times, respectively, of the design earthquake (72-year). Maximum values of the axial forces and bending moments obtained for the Elazığ-Sivrice earthquake in the middle part of the pylon increase by 3.22 and 4.29 times of the design earthquake (72-year).
- For the Elazığ-Sivrice earthquake, maximum cable forces occurred in the longest cables, 213 and 113, of the back span anchorage block and main span deck increase as 3.73 and 4.21 times, respectively.
- Cable forces calculated for both earthquakes are within allowable limits.
- It can be noted that there is no difference between the project values and the geodetic measurements of the deck, pylon and cable sags before and after the Elazığ-Sivrice earthquake. No damage was observed in the deck, the pylon, cables and the connections.
- The results demonstrate that cable-stayed bridges are conservatively designed.

Acknowledgements The authors would like to express sincere thanks to General Directorate of Highways, the 8th Regional Directorate of Highways, Yüksel Proje Inc., Wiecon Co., Doğuş Inc. and Gülsan Inc. for their contributions.

Funding The authors declare that no funds, grants, or other support were received during the preparation of this manuscript.

Declarations

Conflict of interest The authors declare that they have no conflict of interest.

References

AASHTO LRFD (2007) Bridge design specifications. AASHTO, Washington, DC
AFAD (2020) Elazığ-Sivrice Earthquake Report, Disaster and Emergency Management Authority (AFAD). Ankara, Turkey (in Turkish)
Atmaca B, Ates S (2012) Construction stage analysis of three-dimensional cable-stayed bridges. Steel Compos Struct 12(5):413–426
Bayraktar A, Ashour A, Karadeniz H, Kurşun A, Erdiş A (2019) Structural performance of Nissibi cable-stayed bridge during the main and aftershocks of Adıyaman-Samsat earthquake on March 2, 2017. Asian J Civ Eng. https://doi.org/10.1007/s42107-019-00118-0
Bayraktar A, Erdiş A, Kurşun A, Taş Y, Özdilek Y (2023) Final-state structural behavior of the long-span Kömürhan cable-stayed bridge under torsional and bending loadings. J Perform Constr Facil 37(1):04022076
Bozkurt E (2001) Neotectonics of Turkey−a synthesis. Geodin Acta 14:3–30
Camara A (2018) Seismic behavior of cable-stayed bridges: A review. MOJ Civ Eng 4(3):161–169
CEN (European Committee for Standardization) (2004), Design of concrete structures—Part 1.1. Eurocode 2. Brussels, Belgium: CEN.
CEN (European Committee for Standardization), (2005), Design of steel structures—Part 1.1. Eurocode 3. Brussels, Belgium: CEN.
Chang KC, Mo YL, Chen CC, Lai LC, Chou CC (2004) Lessons learned from the damaged Chi-Lu cable-stayed bridge. J Bridg Eng 9:343–352
Chengfeng X, Laijun L, Fangwen W, Caofang Y (2015) Numerical analysis of long span cable-stayed bridge in the construction phase. Open Civ Eng J 9:896–905
Deng X, Liu M (2015) Nonlinear stability analysis of a composite girder cable-stayed bridge with three pylons during construction. Math Prob Eng 2015:1–9
Filiatrauit A, Tinawi R, Massicotte B (1993) Damage to cable-stayed bridge during 1988 Saguenay earthquake. II: dynamic analysis. J Struct Eng 119(5):1450–1463
Gimsing N, Georgakis C (2011) Cable supported bridges: concept and design. John Wiley & Sons, USA
Goto A, Toshimi M, Toshihiro K (1998) Effects of the Hyogo-Ken-Nanbu earthquake on the Akashi Kaikyo bridge, Ein Dienst der ETH-Bibliothek, ETH Zürich. Rämistrasse 101:8092. https://doi.org/10.5169/seals-59870
Granata MF, Longo G, Recupero A, Arici M (2018) Construction sequence analysis of long-span cable-stayed bridges. Eng Struct 174:267–281
Kim H-J, Won D-G, Kang Y-J, Kim S (2017) Structural stability of cable-stayed bridges during construction. Int J Steel Struct 17(2):443–469
Kim S, Won D, Kang Y-J (2019) Ultimate behavior of steel cable-stayed bridges during construction. Int J Steel Struct 19(3):932–951
KOERI (2020) 24 January 2020 (20:55) Elazığ-Sivrice Earthquake Report, Kandilli Observatory and Earthquake Research Institute, 2020. İstanbul, Turkey
Kömürhan Bridge Project (2012) Yüksel Project Inc. Ankara, Turkey
Lee K, Kim S, Choi J, Kang Y (2015) Ultimate behavior of cable stayed bridges under construction: experimental and analytical study. Int J Steel Struct 15(2):311–318
Li H, Ou J (2016) The state of the art in structural health monitoring of cable-stayed bridges. J Civ Struct Heal Monit 6(1):43–67
Ma C, Duan Q, Li Q, Liao H, Tao Q (2019) Aerodynamic characteristics of a long-span cable-stayed bridge under construction. Eng Struct 184:232–246
Martins AMB, Simões LMC, Negrão JHJO (2020) Optimization of cable-stayed bridges: a literature survey. Adv Eng Softw 149:102829. https://doi.org/10.1016/j.advengsoft.2020.102829
METU (2020) Elazığ-Sivrice Earthquake (Mw = 6.8) Reconnaissance Study Report, Middle East Technical University, Earthquake Engineering Research Center, Report No: METU/EERC 2020–01, 2020. Ankara, Turkey

Morgenthal G, Yamasaki Y (2011) Aerodynamic behaviour of very long cable-stayed bridges during construction. Proc Eng 14:1463–1471
Nasu S, Tatsumi M (1995) Effect of the Southern Hyogo earthquake on the Akashi-Kaikyo bridge. Honshu-Shikoku Bridge Authority, Tokyo, Japan
Okuda M, Fukunaga S, Endo K (2009) Seismic design and seismic performance retrofit study for the Akashi Kaikyo Bridge. Bridge Struct 5(2–3):109–118
Park SW, Jung MR, Min DJ, Kim MY (2016) Construction stage analysis of cable-stayed bridges using the unstrained element length method. J Korean Soc Civil Eng 36(6):991–998
Patel M, Thomas M, Sodha AH (2017) Construction stage analysis of cable stayed bridge. Int J Tech Innovat Modern Eng Sci (IJTIMES) 3(3):13487–13496
Pipinato A, Pellegrino C, Modena C (2012) Structural analysis of the cantilever construction process in cable-stayed bridges. Periodica Polytech Civ Eng 56(2):141–166
Purohit KH, Bage AA (2017) Construction stage analysis of cable stayed bridge by cantilever method of construction (Nagpur Cable Stayed Bridge). Int J Innovat Res Sci, Eng Technol 6(7):13487–13496
SAP2000 (2010), Computers and Structures Inc., USA.
Siringoringo DM, Fujino Y (2006) Observed dynamic performance of the Yokohama-Bay Bridge from system identification using seismic records. Struct Control Health Monit 13:226–244
Siringoringo DM, Fujino Y (2007) Dynamic characteristics of a curved cable-stayed bridge identified from strong motion records. Eng Struct 29:2001–2017
Siringoringo DM, Fujino Y, Namikawa K (2014) Seismic response analyses of the Yokohama bay cable-stayed bridge in the 2011 great east Japan earthquake. J Bridg Eng 19(8):A4014006
Su C, Fan X, He T (2007) Wind-induced vibration analysis of a cable-stayed bridge during erection by a modified time-domain method. J Sound Vib 303(1–2):330–342
Svensson H (2012) Cable-stayed Bridges. Ernst and Sohn Company, USA
Tada K, Jin H, Kitagawa M, Nitta A, Toriumi R (1995) Effect of the Southern Hyogo Earthquake on the Akashi-Kaikyo Bridge. Struct Eng Int 5(3):179–181. https://doi.org/10.2749/101686695780601079
TEC (2007) Turkish earthquake code. Ministry of Public Works and Settlement, Ankara, Turkey
Tsompanakis Y (2014) Earthquake return period and its incorporation into seismic actions. Encyclopedia Earthq Eng. https://doi.org/10.1007/978-3-642-36197-5_116-1
URL-1 (2021), https://tadas.afad.gov.tr/map, 01.01.2021.
Wang P-H, Tang T-Y, Zheng H-N (2004) Analysis of cable-stayed bridge at different erection stages during construction using cantilever method. Comput Struct 82(4–5):329–346
Wilson JC, Holmes K (2007) Seismic vulnerability and mitigation during construction of cable-stayed bridges. J Bridg Eng 12(3):364–372
Yadi S, Suhendro B, Priyosulistyo H, Aminullah A (2018) Shake table test of floating cable-stayed bridge under earthquake excitation during construction with balanced cantilever method. Int J Civ Eng Technol 9(11):2063–2081
Yamagata M, Yasuda M, Nitta A, Yamamoto S (1996) Effects on the Akashi Kaikyo Bridge. Special Issue Soils Found 36:179–187
Yasuda, M., Kitagawa, M., Toritni, M. and Fukunaga, S. (2000), Seismic design and behavior during the Hyogo-Ken Nanbu earthquake of the Akashi Kaikyo bridge. In: 12 WCEE 2000: 12th World Conference on Earthquake Engineering; Auckland, New Zeland.
Yi J, Li J (2019) Experimental and numerical study on seismic response of inclined tower legs of cable-stayed bridges during earthquakes. Eng Struct 183:180–194
YP (2020), Preliminary inspection report for Kömürhan Bridge regarding the Sivrice (Elazığ) Earthquake, Yüksel Project, Ankara, Turkey (in Turkish).

Authors and Affiliations

Alemdar Bayraktar[1] · Altok Kurşun[2] · Arif Erdiş[2] · Mehmet Akköse[1] · Yavuzhan Taş[3] · Tony T. Y. Yang[4]

✉ Alemdar Bayraktar
alemdarbayraktar@gmail.com

Altok Kurşun
altok.kursun@gulsanholding.com.tr

Arif Erdiş
arif.erdis@gulsanholding.com.tr

Mehmet Akköse
akkosemehmet@gmail.com

Yavuzhan Taş
ytas@kgm.gov.tr

Tony T. Y. Yang
yang@civil.ubc.ca

[1] Karadeniz Technical University, Trabzon, Turkey

[2] Gülsan Inc., Istanbul, Turkey

[3] General Directorate of Highways, Elazığ, Turkey

[4] Department of Civil Engineering, The University of British Columbia, Vancouver, Canada